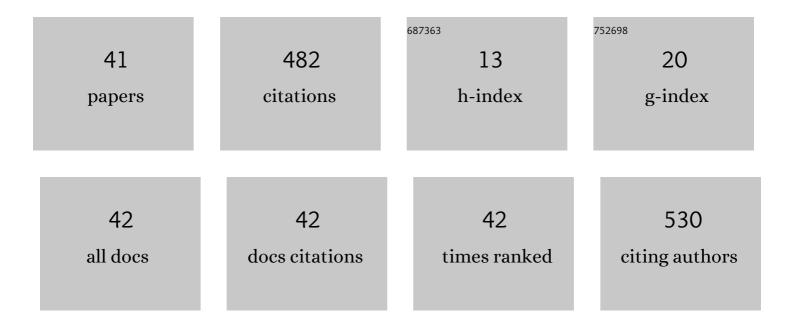
Takahiro Ohkubo

List of Publications by Year in descending order

Source: https://exaly.com/author-pdf/1526801/publications.pdf Version: 2024-02-01



#	Article	IF	CITATIONS
1	Formation of metallic cation-oxygen network for anomalous thermal expansion coefficients in binary phosphate glass. Nature Communications, 2017, 8, 15449.	12.8	42
2	Pore distribution of water-saturated compacted clay using NMR relaxometry and freezing temperature depression; effects of density and salt concentration. Applied Clay Science, 2016, 123, 148-155.	5.2	33
3	An approach of NMR relaxometry for understanding water in saturated compacted bentonite. Physics and Chemistry of the Earth, 2008, 33, S169-S176.	2.9	29
4	Molecular dynamics simulations of Nafion and sulfonated polyether sulfone membranes. I. Effect of hydration on aqueous phase structure. Journal of Molecular Modeling, 2011, 17, 739-755.	1.8	26
5	Insights from abÂinitio molecular dynamics simulations for a multicomponent oxide glass. Journal of the American Ceramic Society, 2018, 101, 1122-1134.	3.8	21
6	Molecular dynamics simulations of nafion and sulfonated poly ether sulfone membranes II. Dynamic properties of water and hydronium. Journal of Molecular Modeling, 2012, 18, 533-540.	1.8	20
7	Examination of structure and optical properties of Ce3+-doped strontium borate glass by regression analysis. Scientific Reports, 2021, 11, 3811.	3.3	19
8	An adaptive finite-element method for large-scale ab initio molecular dynamics simulations. Physical Chemistry Chemical Physics, 2015, 17, 31444-31452.	2.8	18
9	First-Principles Molecular Dynamics Simulation and Conductivity Measurements of a Molten xLi2O–(1) Tj ETQo	q1 <u>1 0</u> .784	4314 rgBT / <mark>)</mark> 17
10	Molecular Dynamics Simulation of Water Confinement in Disordered Aluminosilicate Subnanopores. Scientific Reports, 2018, 8, 3761.	3.3	17
11	Modeling the Structure and Dynamics of Lithium Borosilicate Glasses with Ab Initio Molecular Dynamics Simulations. Journal of Physical Chemistry C, 2021, 125, 8080-8089.	3.1	17
12	<i>Ab Initio</i> Molecular Dynamics Simulations and GIPAW NMR Calculations of a Lithium Borate Glass Melt. Journal of Physical Chemistry B, 2016, 120, 3582-3590.	2.6	15
13	Photocatalytic hydrogen generation of monolithic porous titanium oxide-based glass–ceramics. Scientific Reports, 2020, 10, 11615.	3.3	15
14	New Insights into the Cs Adsorption on Montmorillonite Clay from 133Cs Solid-State NMR and Density Functional Theory Calculations. Journal of Physical Chemistry A, 2018, 122, 9326-9337.	2.5	13
15	Temperature-Dependent Water Redistribution from Large Pores to Fine Pores after Water Uptake in Hardened Cement Paste. Journal of Advanced Concrete Technology, 2020, 18, 588-599.	1.8	13
16	Correlation between emission properties, valence states of Ce and chemical compositions of alkaline earth borate glasses. Journal of Luminescence, 2018, 197, 98-103.	3.1	12
17	Conduction Mechanism in 70Li ₂ S-30P ₂ S ₅ Glass by Ab Initio Molecular Dynamics Simulations: Comparison with Li ₇ P ₃ S ₁₁ Crystal. ACS Applied Materials & Interfaces, 2020, 12, 25736-25747.	8.0	12
18	Modified Li ₇ P ₃ S ₁₁ Glass-Ceramic Electrolyte and Its Characterization. ACS Applied Materials & Interfaces, 2021, 13, 37071-37081.	8.0	12

Таканіго Онкиво

#	Article	IF	CITATIONS
19	Deconvolution and Estimation of Water Diffusion in Sulfonated Polyethersulfone Membranes Using Diffusion-Weighted Inversion Recovery Journal of Physical Chemistry Letters, 2012, 3, 1030-1034.	4.6	11
20	Diffusion of tritiated water, 137Cs+, and 125Iâ^' in compacted Ca-montmorillonite: Experimental and modeling approaches. Applied Clay Science, 2021, 211, 106176.	5.2	11
21	Correlation between Structures and Physical Properties of Binary ZnO–P ₂ O ₅ Glasses. Physica Status Solidi (B): Basic Research, 2020, 257, 2000186.	1.5	10
22	Low melting oxide glasses prepared at a melt temperature of 500°C. Scientific Reports, 2021, 11, 214.	3.3	10
23	Li conduction pathways in solid-state electrolytes: Insights from dynamics and polarizability. Chemical Physics Letters, 2018, 698, 234-239.	2.6	9
24	X-ray absorption near-edge structure of Ag cations in phosphate glasses for radiophotoluminescence applications. Journal of the Ceramic Society of Japan, 2019, 127, 924-930.	1.1	9
25	Self-diffusion coefficient of lithium in molten xLi2O–(1â^'x)B2O3 system using high-temperature PFG NMR. Chemical Physics Letters, 2012, 530, 61-63.	2.6	8
26	Magnesiothermic Reduction of Silicon Dioxide to Obtain Fine Silicon Powder in Molten Salt Media: Analysis of Reduction Mechanism. Electrochemistry, 2018, 86, 198-201.	1.4	8
27	Lithium conduction and the role of alkaline earth cations in Li2S–P2S5–MS (M = Ca, Sr, Ba) glasses. Journal of Non-Crystalline Solids, 2020, 538, 120025.	3.1	8
28	Pore distribution of compacted Ca-montmorillonite using NMR relaxometry and cryoporometry: Comparison with Na-montmorillonite. Microporous and Mesoporous Materials, 2021, 313, 110841.	4.4	8
29	A new universal force-field for the Li ₂ S–P ₂ S ₅ system. Physical Chemistry Chemical Physics, 2022, 24, 2567-2581.	2.8	7
30	Changes in surface structure of sodium aluminoborosilicate glasses during aqueous corrosion analyzed by using NMR. Journal of Physics and Chemistry of Solids, 2015, 77, 164-171.	4.0	6
31	Characterization of irradiation-induced novel voids in α-quartz. AIP Advances, 2020, 10, 125212.	1.3	5
32	Elucidating the Atomic Structures of the Gel Layer Formed during Aluminoborosilicate Glass Dissolution: An Integrated Experimental and Simulation Study. Journal of Physical Chemistry C, 2022, 126, 7999-8015.	3.1	4
33	Understanding properties of copoly(arylene ether nitrile)s high-performance polymer electrolyte membranes for fuel cells from molecular dynamics simulations. Theoretical Chemistry Accounts, 2011, 130, 555-561.	1.4	3
34	Molecular Dynamics Simulations of the Thermal and Transport Properties of Molten NaNO ₂ –NaNO ₃ Systems. Electrochemistry, 2018, 86, 104-108.	1.4	3
35	Structural analyses of amorphous calcium carbonate before and after removing strontium ions from an aqueous solution. Journal of the Ceramic Society of Japan, 2022, 130, 225-231.	1.1	3
36	The Local Structure of Liquid TiCl4 Analyzed by X-Ray Diffraction and Raman Spectroscopy. Zeitschrift Fur Naturforschung - Section A Journal of Physical Sciences, 2013, 68, 66-72.	1.5	2

Таканіго Онкиво

#	Article	IF	CITATIONS
37	Densities and Refractive Indices of Molten Alkali Iodides: Estimation of Electronic Polarizability of an Iodide Ion. Journal of Chemical & Engineering Data, 2020, 65, 5240-5248.	1.9	2
38	Activity Report on Information-Gathering of Database Literatures for Molten Salts. Electrochemistry, 2020, 88, 243-252.	1.4	2
39	Time-dependent Born charges of lithium borate melts by ab initio molecular dynamics. Chemical Physics Letters, 2014, 612, 68-72.	2.6	1
40	Electronic Polarisability of NaNO ₂ –NaNO ₃ and NaOH–NaNO ₃ Ionic Melts and Effective Ionic Radius of OH ^{ï¼} . Zeitschrift Fur Naturforschung - Section A Journal of Physical Sciences, 2017, 72, 71-76.	1.5	1
41	Electrical Conductivity of Molten DyCl3-NaCl and DyCl3-KCl Systems: An Approach to Structural Interpretations of Rare Earth Chloride Melts. Zeitschrift Fur Naturforschung - Section A Journal of Physical Sciences, 2017, 72, 1105-1112.	1.5	0